

## Indian Ocean Dipole Overrides ENSO's Influence on Cool Season Rainfall across the Eastern Seaboard of Australia

A. PEPLER

*Climate Information Services, Bureau of Meteorology, and Centre of Excellence for Climate Systems Science and Climate Change Research Centre, University of New South Wales, Sydney, New South Wales, Australia*

B. TIMBAL

*Centre for Australian Weather and Climate Research, Bureau of Meteorology, Melbourne, Victoria, Australia*

C. RAKICH

*Climate Information Services, Bureau of Meteorology, Melbourne, Victoria, Australia*

A. COUTTS-SMITH

*Climate Information Services, Bureau of Meteorology, Sydney, New South Wales, Australia*

(Manuscript received 8 September 2013, in final form 21 January 2014)

### ABSTRACT

The strong relationship between eastern Australian winter–spring rainfall and tropical modes of variability such as the El Niño–Southern Oscillation (ENSO) does not extend to the heavily populated coastal strip east of the Great Dividing Range in southeast Australia, where correlations between rainfall and Niño-3.4 are insignificant during June–October. The Indian Ocean dipole (IOD) is found to have a strong influence on zonal wind flow during the winter and spring months, with positive IOD increasing both onshore winds and rainfall over the coastal strip, while decreasing rainfall elsewhere in southeast Australia. The IOD thus opposes the influence of ENSO over the coastal strip, and this is shown to be the primary cause of the breakdown of the ENSO–rainfall relationship in this region.

### 1. Introduction

Across most of eastern Australia, the interannual variability of rainfall is strongly moderated by modes of naturally occurring tropical variability in the Pacific and Indian Oceans. The most frequently discussed influence is the El Niño–Southern Oscillation (ENSO; e.g., [McBride and Nicholls 1983](#); [Nicholls 1985](#); [Power et al. 1998](#)), while the Indian Ocean dipole (IOD; [Saji et al. 1999](#)) has also been demonstrated to play a major role. When the influences of these two drivers are combined into a single index of tropical SST variability such as the tropical tripole index ([Timbal and Hendon 2011](#)) they are responsible for

more than 20% of rainfall variability in southeast Australia (SEA) in the cool season ([Fig. 1](#)).

There has been substantial research in recent years as to the influence and interactions of the IOD and ENSO on southeast Australian rainfall (e.g., [Meyers et al. 2007](#); [Ummenhofer et al. 2009a,b, 2011](#); [Cai et al. 2011, 2012](#); [Risbey et al. 2009a,b](#)). These studies have consistently demonstrated that positive IOD (pIOD) is the major feature of droughts in southeastern Australia, with El Niño playing a lesser role. [Cai et al. \(2011, 2012\)](#) in particular identified that the influence of ENSO itself is restricted to the subtropics during winter and spring, with teleconnections through the Indian Ocean being the major influence on rainfall patterns in southern Australia. However, while these papers have performed analyses over the entirety of Australia, detailed discussion has focused on the key agricultural regions of southeast Australia, south of 35°S.

---

*Corresponding author address:* Acacia Pepler, Climate Change Research Centre, University of New South Wales, Sydney, NSW 2052, Australia.  
E-mail: a.pepler@student.unsw.edu.au

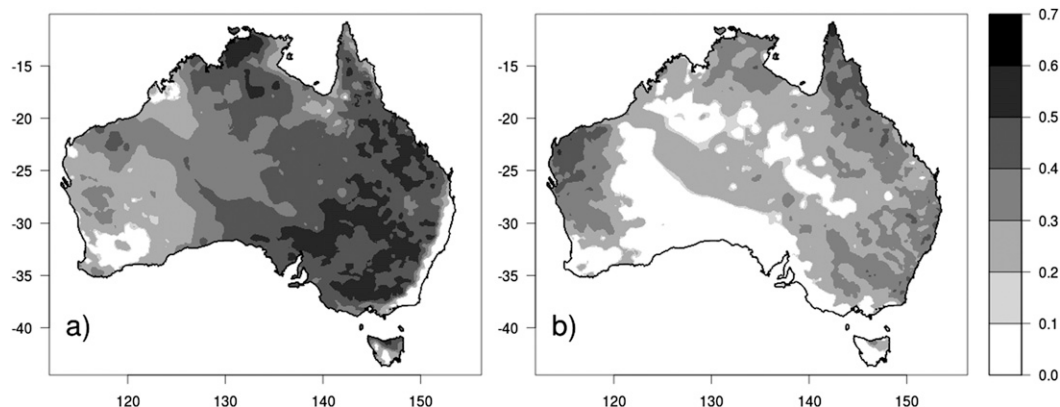


FIG. 1. Correlation between the [Timbal and Hendon \(2011\)](#) tropical tripole index and Australian rainfall (1900–2012) during (a) June–October and (b) November–March. Only correlations that are statistically significant at the 95% level are shown.

The eastern seaboard of Australia (ESB) can be defined as the region of southeast Australia bounded by the Great Dividing Range to the west and the Pacific Ocean to the east ([Timbal 2010](#); [Fig. 2](#)). This region exhibits distinctly different rainfall patterns to elsewhere in southeast Australia; notably, the relationship between tropical SST variations and cool season (June–October) rainfall appears to be weak or absent in this region (e.g., [McBride and Nicholls 1983](#); [Fig. 1](#)). This is not the case during the warm season (November–March), when the relationship between ENSO and rainfall is strongest on the coastal strip. As this region includes

two of Australia’s largest cities (Sydney and Brisbane) and their associated water supplies, understanding the drivers of current rainfall variability is critical for decision making in this region.

Previous research identified east coast lows (ECLs), intense coastal lows off the east coast, as a potential cause of this variation ([Pepler et al. 2014](#)). However, while ECLs are a major contributor to rainfall variability in this region and show little variability related to tropical climate drivers, removing the ECL-related signal in rainfall data did not fully explain the absence of ENSO relationships in this region, particularly in the

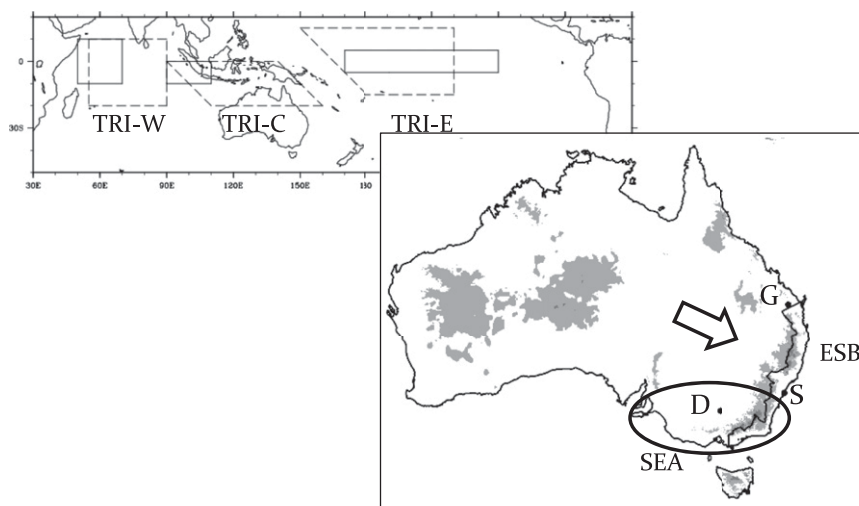


FIG. 2. The Indo-Pacific tropics, with the DMI (Indian Ocean) and Niño-3.4 (Pacific Ocean) averaging regions indicated with solid lines and the regions used for calculating the tropical tripole index (TRI) indicated with dashed lines. Inset shows the Australian Great Dividing Range, with elevation shaded using 500 m and an outline of the ESB region. Sydney (S), Gayndah (G), and Deniliquin (D) are shown, with an arrow indicating the “zonal winds” represented by the GDI. An oval indicates the region of SEA typically investigated in SEA rainfall studies.

TABLE 1. List of years by BoM ENSO and IOD classification, 1958–2012.

	pIOD	Neutral	nIOD
El Niño	1964, 1972, 1977, 1982, 1994, 1997, and 2006	1965, 1969, 1987, 1991, 2002, and 2009	1993
Neutral	1961, 1967, 1983, and 2012	1959, 1962, 1966, 1968, 1976, 1978, 1979, 1980, 1981, 1984, 1985, 1986, 1990, 1995, 2001, 2003, 2004, and 2005	1958, 1960, 1989, 1992, and 1996
La Niña	2007 and 2011	1970, 1973, 1988, 1998, 1999, 2000, and 2008	1964, 1971, 1974, 1975, and 2010

northern ESB. Instead, research has found a stronger relationship between ESB rainfall and atmospheric circulation such as the southern annular mode (e.g., Hendon et al. 2007; Speer et al. 2011) and associated zonal wind flow anomalies (Rakich et al. 2008), particularly during the summer months.

This paper focuses on the relationship among ENSO, the IOD, and zonal wind anomalies across southeast Australia and how these impact rainfall patterns on the ESB. We first quantify the relationship between zonal wind anomalies and rainfall on the ESB, which are markedly different to those in southeast Australia west of the Great Dividing Range. We then identify the influences of both ENSO and the IOD on zonal wind anomalies and moisture fluxes, noting a significantly stronger influence from the IOD. Finally, we discuss the implications for Australian rainfall and demonstrate that the interaction of the IOD with ENSO is a major influence of the ENSO–rainfall relationship along the east coast.

## 2. Data

Sea surface temperature (SST) anomalies were computed for 1900–2012 using the Met Office Hadley Centre SST analyses interpolated on a  $1^\circ \times 1^\circ$  grid (Rayner et al. 2006). This was used to calculate the monthly Niño-3.4 (an index of ENSO) and dipole mode index (DMI), an index of the IOD (e.g., Saji et al. 1999), and the Timbal and Hendon (2011) tropical tripole index, the difference between sea surface temperatures to the north of Australia and the average of the equatorial Indian Ocean and central Pacific; averaging regions are shown in Fig. 2.

The ENSO and IOD statuses for each year since 1958 are given in Table 1, based on the official event classifications of the Bureau of Meteorology (BoM; the classifications are available at [www.bom.gov.au/climate/ens/ensorain.comp.shtml](http://www.bom.gov.au/climate/ens/ensorain.comp.shtml) and [www.bom.gov.au/climate/IOD/](http://www.bom.gov.au/climate/IOD/)). Results are relatively robust to the choice of classification scheme, with similar outcomes using the classification of Meyers et al. (2007) and Ummenhofer

et al. (2009a, 2011). The monthly Southern Oscillation index (SOI) was also retrieved from the BoM (at [www.bom.gov.au/climate/current/soihtm1.shtml](http://www.bom.gov.au/climate/current/soihtm1.shtml)).

The zonal wind anomalies were represented by the Gayndah–Deniliquin index (GDI; Rakich et al. 2008). This is a measure of the difference between 0900 local time (LT) mean sea level pressure (MSLP) at Gayndah (25.6°S, 151.6°E) and Deniliquin (35.6°S, 145.0°E), two long-record sites spanning the latitudinal range of southeast Australia. The GDI is a representation of daily and monthly zonal geostrophic wind flow into this region, calculated since 1893, with both daily and monthly values derived. Days are designated “easterly” where the values of the index are positive with 0900 LT MSLP higher at Deniliquin and “westerly” where the index is negative with 0900 LT MSLP higher at Gayndah. Positive GDI anomalies therefore reflect anomalously easterly zonal wind flow.

Monthly vertically integrated moisture flux anomalies were computed for 1958–2012 using the National Centers for Environmental Prediction–National Center for Atmospheric Research (NCEP–NCAR) reanalyses (Kalnay et al. 1996). We computed the zonal and meridional components of moisture fluxes as the multiple of the specific humidity and the  $u$  and  $v$  components of wind velocity, vertically integrated across all levels between 1000 and 500 hPa.

Daily gridded rainfall data from the Australian Water Availability Project (AWAP; Jones et al. 2009) were used for monthly and seasonal correlations; these can be obtained by request from the BoM. AWAP was also used to create datasets of the seasonal rainfall associated with easterly or westerly wind flows, with all rainfall recorded to 0900 LT on a day where the daily GDI was positive attributed to easterly flow.

Throughout this paper, “cool season” refers to the months June–October and “warm season” refers to November–March, and statistical significance is assessed at the 95% level. This paper does not address rainfall anomalies in April and May, as the standard deviation of Niño-3.4 is lowest in these months and ENSO events typically end by March (e.g., Trenberth 1997).

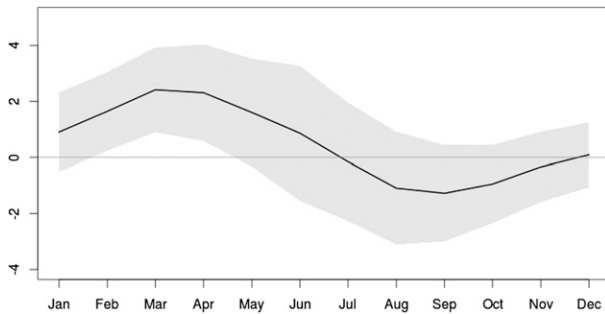


FIG. 3. Monthly average and standard deviation of the GDI, 1900–2012.

### 3. GDI and east Australian rainfall

Because of the proximity of the warm Pacific Ocean, easterly winds increase moisture advection into the coastal region and consequently enhance rainfall along the ESB. This region is bounded by the Great Dividing Range, a mountain range which lies approximately perpendicular to the zonal wind flow and acts as an impediment to rain-bearing systems (Fig. 2); westerly driven systems such as cold fronts can produce rainfall across much of southeast Australia, particularly on the western slopes of the divide because of orographic forcing, but are less likely to produce rainfall to the east of the ridgeline owing to subsidence. As a consequence, the Great Dividing Range acts as a clear boundary for weather regimes, with the relationship between rainfall and zonal wind anomalies differing between areas east and west of the divide.

The seasonal GDI is a representation of the relative dominance of easterly or westerly zonal flow in southeast Australia. Annually, the mean GDI is +0.49, reflecting prevailing easterly values for much of the year.

The prevailing wind direction is easterly on 57% of days between 1900 and 2012; these days were responsible for more than 70% of rainfall along the ESB but less than 30% of rainfall in much of the remaining areas of Australia south of 30°S and east of 130°E.

The annual average GDI shows pronounced interannual variability, with a standard deviation of 2.1, in addition to strong seasonality (Fig. 3). The geostrophic flow is predominantly easterly during the warm season, when the subtropical ridge is in its southernmost position and easterly flow is experienced on 60% of days, with a seasonal GDI of +0.94. The fraction of easterly winds is reduced to 50% of days during June–October, with a seasonal average GDI of –0.55.

During the cool season, westerly and easterly daily wind anomalies are similar in frequency. However, days with easterly zonal flow are responsible for over 60% of cool season rainfall in the ESB but less than 30% of cool season rainfall in much of southeast Australia west of the divide (Fig. 4a). This is consistent with results by Risbey et al. (2009a), which identified that more than 80% of cool season rainfall in western southeast Australia is associated with either cold fronts or cutoff lows, both of which are typically embedded in westerly flow. As a consequence, enhanced easterly flow is associated with increased rainfall on the ESB but decreased rainfall west of the divide, so correlations between rainfall and the GDI are of opposite sign east and west of the Great Dividing Range (Fig. 4b).

### 4. Tropical climate indices and wind anomalies

Rakich et al. (2008) observed a positive correlation between the GDI and SOI during summer, with La Niña years associated with enhanced easterly wind flow; in contrast, Jones and Trewin (2000) and others observed

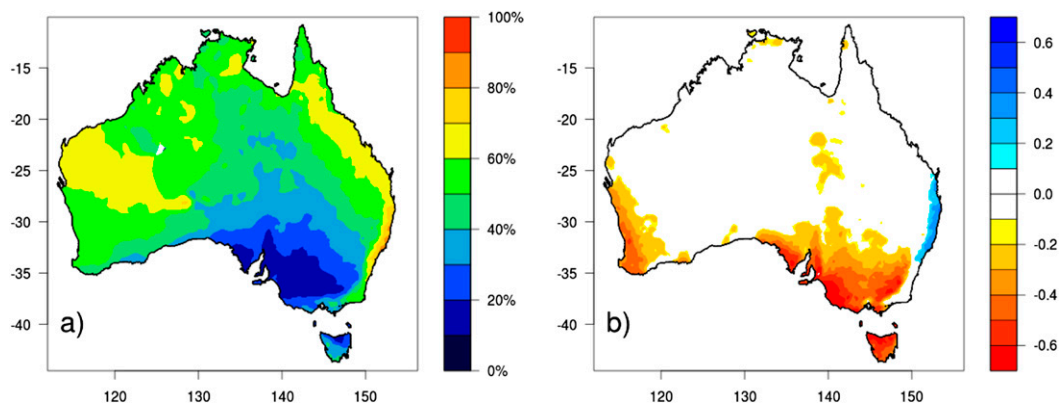


FIG. 4. (a) Percentage of June–October rainfall associated with positive daily GDI and (b) correlation between June–October GDI and rainfall, 1900–2012. Only correlations that are statistically significant at the 95% level are shown.

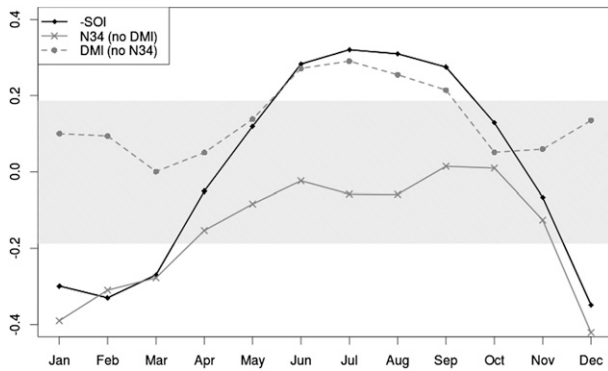


FIG. 5. Three-month running correlations between the GDI and the (inverse) SOI, 1900–2012. Three-month running partial correlations between the GDI and each of Niño-3.4 and DMI are shown, to indicate independent ENSO and IOD influences. Gray shading indicates correlations that are not statistically significant.

that El Niño years are associated with easterly wind anomalies during winter. These contrasting results reflect a strong seasonal variation in the relationship between ENSO and zonal winds, with positive correlations between the GDI and the SOI during the warm season and negative correlations during the cool season (Fig. 5). This seasonal variation is clearly related to the strikingly disparate seasonal patterns of the ENSO influence on rainfall to the east and west of the Great Divide, with strong correlations only to the west of the divide during the cool season but east of the divide in the warm season (Fig. 1). This then raises the question of what mechanism can explain this observed reversal in influence.

Several studies in recent years have sought to decompose the relationship among the IOD, ENSO, and southeast Australian rainfall (e.g., Meyers et al. 2007; Ummenhofer et al. 2009a, 2011; Risbey et al. 2009a,b). These have typically focused on a region of southeast Australia south of 35°S, with the IOD found to be a major driver of rainfall variability in this region. Cai et al. (2011, 2012) have discussed the interaction of ENSO and IOD in terms of two main teleconnections; a tropical connection related to the impacts of the Southern Oscillation in northeast Australia, and a subtropical connection modulated through the Indian Ocean. These papers identified the subtropical teleconnection as the main influence on rainfall in southern Australia during the later part of the cool season. This furthers research from Meyers et al. (2007) and Ummenhofer et al. (2009a), who identified the Indian Ocean dipole as a major driver of SEA rainfall during the austral winter and spring. However, it is important to note that the IOD and ENSO are strongly correlated, particularly during austral spring (September–November), and thus their impacts cannot be fully separated.

TABLE 2. Average June–October GDI, 1958–2012, for the ENSO–IOD classifications given in Table 1.

	pIOD	Neutral	nIOD
El Niño	0.77	−0.49	—
Neutral	0.32	−0.60	−0.90
La Niña	—	−0.31	−0.95

As ENSO and IOD interact strongly, with positive IOD and El Niño years tending to occur in concert, we used partial correlations to isolate the relationship between zonal winds (GDI) and each driver in the absence of the other (Fig. 5). During the cool season, the majority of the relationship between tropical climate drivers and zonal wind flow appears to be driven by the IOD, with the partial correlations between Niño-3.4 and GDI close to zero, but statistically significant correlations between the GDI and DMI. This is clear from the average June–October GDI for various ENSO–IOD states (Table 2): in the absence of an IOD event, the June–October mean GDI is similar to neutral conditions for both El Niño and La Niña years. In comparison, negative IOD (nIOD) years show an enhancement of the average westerly flow, while, on average, positive IOD years exhibit prevailing easterly wind flow, regardless of ENSO state. This suggests IOD is a dominating influence over ENSO in the SEA domain.

In contrast, during the warm season, the standard deviation of the DMI is low (e.g., Saji et al. 1999), with the onset of the monsoon acting to end IOD events (e.g., Meyers et al. 2007, Taschetto et al. 2011). The strict seasonality of the dominating IOD influence, constrained only to the cool season, explains the starkly different relationship between ENSO and zonal winds in the warm and cool seasons, demonstrated in Fig. 5.

To better understand the interactions between ENSO and IOD in terms of physical changes to circulation patterns and moisture sources, and to consequently better understand associated rainfall patterns, we investigate changes in the vertically integrated moisture flux. During the cool season, the prevailing circulation is westerly in southern Australia and easterly in northern Australia, with a strong moisture flux toward the Maritime Continent (Fig. 6).

During the June–October period, Ummenhofer et al. (2009a) noted that positive IOD events are associated with significant easterly moisture flux anomalies over the Australian continent in southeast Australia, while negative IOD events are associated with strong westerly moisture flux anomalies from the Indian Ocean into the continent. These patterns are consistent with the moisture flux anomalies associated with extreme dry and wet periods for southeast Australia (south of 35°S), respectively (Ummenhofer et al. 2011), with air parcels

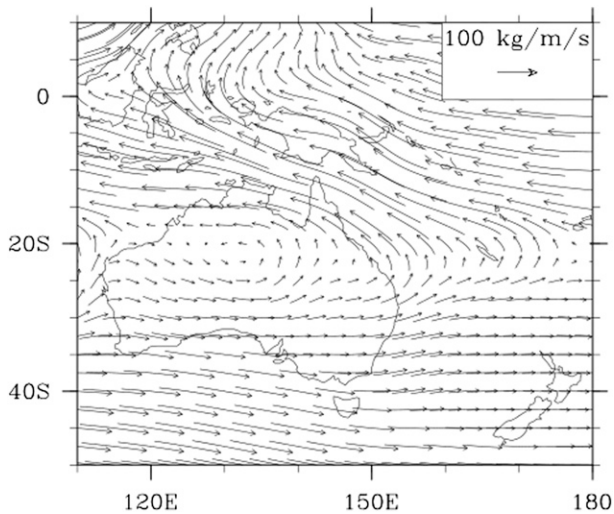


FIG. 6. Average moisture flux, vertically integrated between 1000 and 500 hPa, across the Australian region during the cool season (June–October), 1958–2012.

with trajectories originating in the Indian Ocean substantially more likely to cause rain in southeast Australia west of the Great Dividing Range (e.g., [Brown et al. 2009](#); [McIntosh et al. 2012](#)).

When the influences of ENSO and the IOD are separated ([Figs. 7e,f](#)), positive IOD events are associated with anomalous southeasterly moisture flux anomalies across most of the Australian landmass, regardless of ENSO state. This weakens the prevailing westerly circulation and consequently the moisture source to western southeast Australia. However, along the eastern seaboard, this acts as an enhanced source of tropical moisture from the warm western Pacific and Tasman Sea. In contrast, negative IOD events are associated with a strengthening of the westerly flow and enhanced rainfall in western southeast Australia, with subsiding offshore winds and drier conditions over the ESB.

In the absence of a corresponding IOD event, the strongest signal of ENSO ([Figs. 7a,b](#)) is apparent in the tropical Pacific, with enhanced trade winds during La Niña events and weakened winds in El Niño events. Across the Australian continent, moisture flux anomalies are generally weak; easterly anomalies along the east coast are apparent in both instances, turning northeasterly inland. However, in the La Niña case, the easterly flow affecting eastern Australia is connected to the tropical western Pacific Ocean and hence indicates an enhanced moisture flux from the tropical western Pacific into northeastern Australia, with little penetration of anomalies south of 30°S. This is consistent with the tropical influence discussed by [Cai et al. \(2011, 2012\)](#), with the June–October influence of ENSO restricted to

northern Australia in the absence of Indian Ocean teleconnections. In contrast, easterly moisture flux anomalies in El Niño years are generally weak and are associated with a northward flux of moisture away from the colder southern Pacific, and hence, they do not contribute to significant moisture transport, with no influence beyond the immediate coastal strip of the ESB.

The combined cases are also informative. The combination of an El Niño event with positive IOD does little to change the IOD-like pattern of easterly wind anomalies across the continent. The only notable change is in the moisture source; in the neutral ENSO–positive IOD case, the moisture flux anomalies are connected to the tropical easterly trade winds, acting as a source of enhanced moisture over the ESB, while in the El Niño positive IOD case, the moisture fluxes are instead from the Tasman Sea. Similarly, when La Niña and negative IOD coincide, the primary moisture source over the Australian continent is westerly anomalies from the warm tropical Indian Ocean, in strong contrast to the easterly wind anomalies observed in the neutral–La Niña case.

## 5. Implications for Australian rainfall

The moisture flux analysis presented in this paper indicates that any impacts of El Niño events in the cool season in SEA are overpowered by the strong relationship between the IOD and zonal wind flow. While IOD and ENSO events frequently occur in concert, the implications of this become visible when the influences of IOD and ENSO on Australian rainfall are separated ([Fig. 8](#)). This analysis is similar to that performed for southeast Australia in recent papers, including [Meyers et al. \(2007\)](#), [Ummenhofer et al. \(2009a, 2011\)](#), and [Risbey et al. \(2009b\)](#), which focused on the rainfall signature of the IOD in southeast Australia south of 35°S. The rainfall patterns shown in the figures are broadly similar to previous studies, reflecting the consistency of results across varying event definitions; however, the strength of the IOD relationship on the coast is stronger than using other definitions, as a result of the smaller selection of IOD events in the BoM database.

Of the six non–La Niña years where IOD was negative since 1958 ([Fig. 8h](#)), only one had above-median rainfall on the east coast between June and October, compared to 5–6 years elsewhere in southeast Australia. In contrast, five of the six non–El Niño positive IOD years ([Fig. 8g](#)) had above-median rainfall on the east coast, but only one year elsewhere in southeast Australia. This rainfall pattern was expected based on the pattern of correlations between GDI and rainfall ([Fig. 3](#)) and the moisture flux anomalies ([Figs. 7e,f](#)).

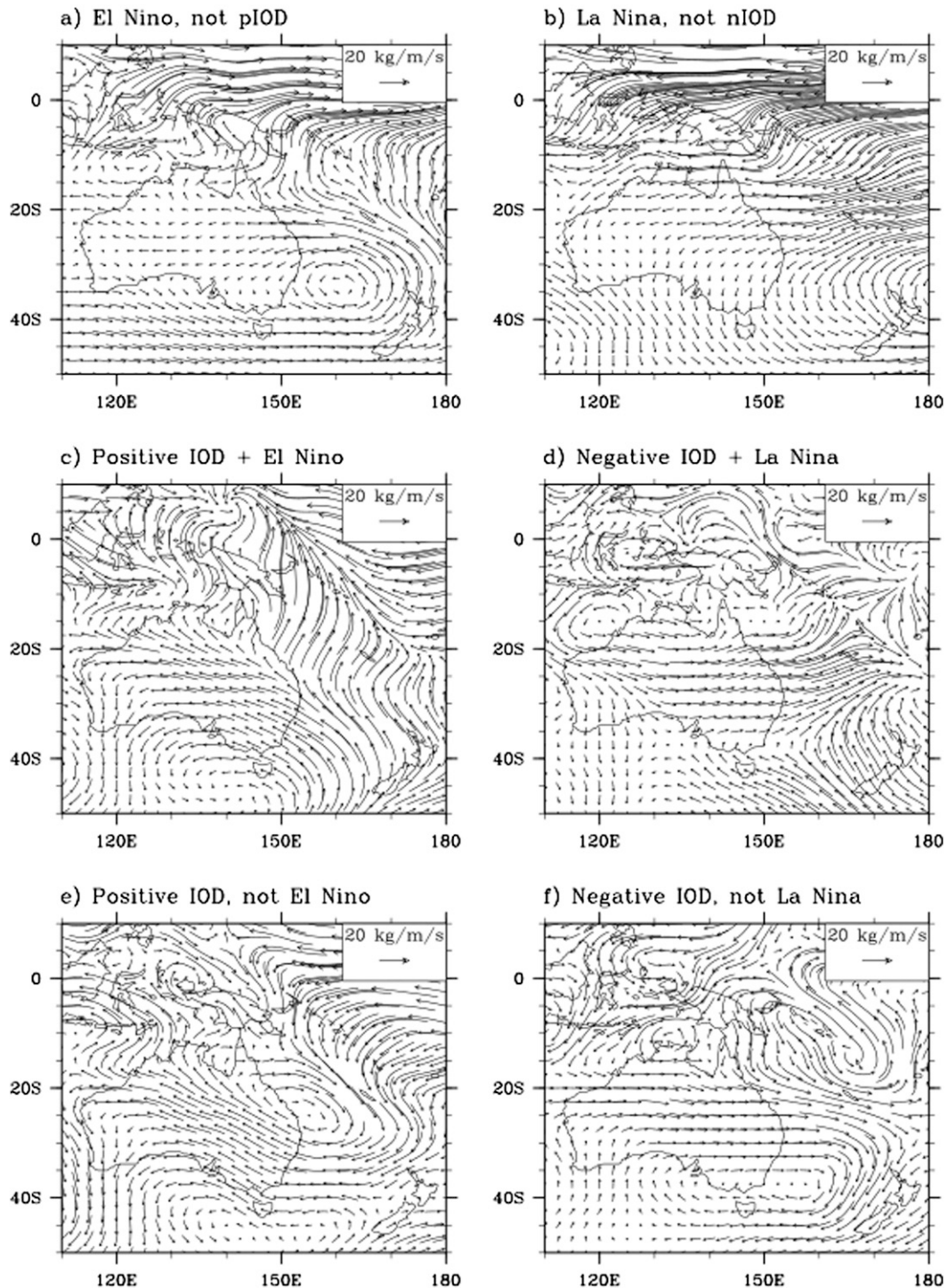


FIG. 7. Composite maps of June–October vertically integrated moisture flux anomalies from the long-term average based on IOD and ENSO events, 1958–2012 (using BoM classification; Table 1).

In comparison, where no IOD event is apparent, the influence of La Niña years is strongest in northeast Australia (Fig. 8d), where easterly moisture flux anomalies are present, while El Niño years have no consistent

impact on southeast Australian rainfall (Fig. 8c); this is also expected from the moisture flux anomalies shown in Fig. 7. It is important to note, however, that strongest rainfall influences in northern Australia are observed

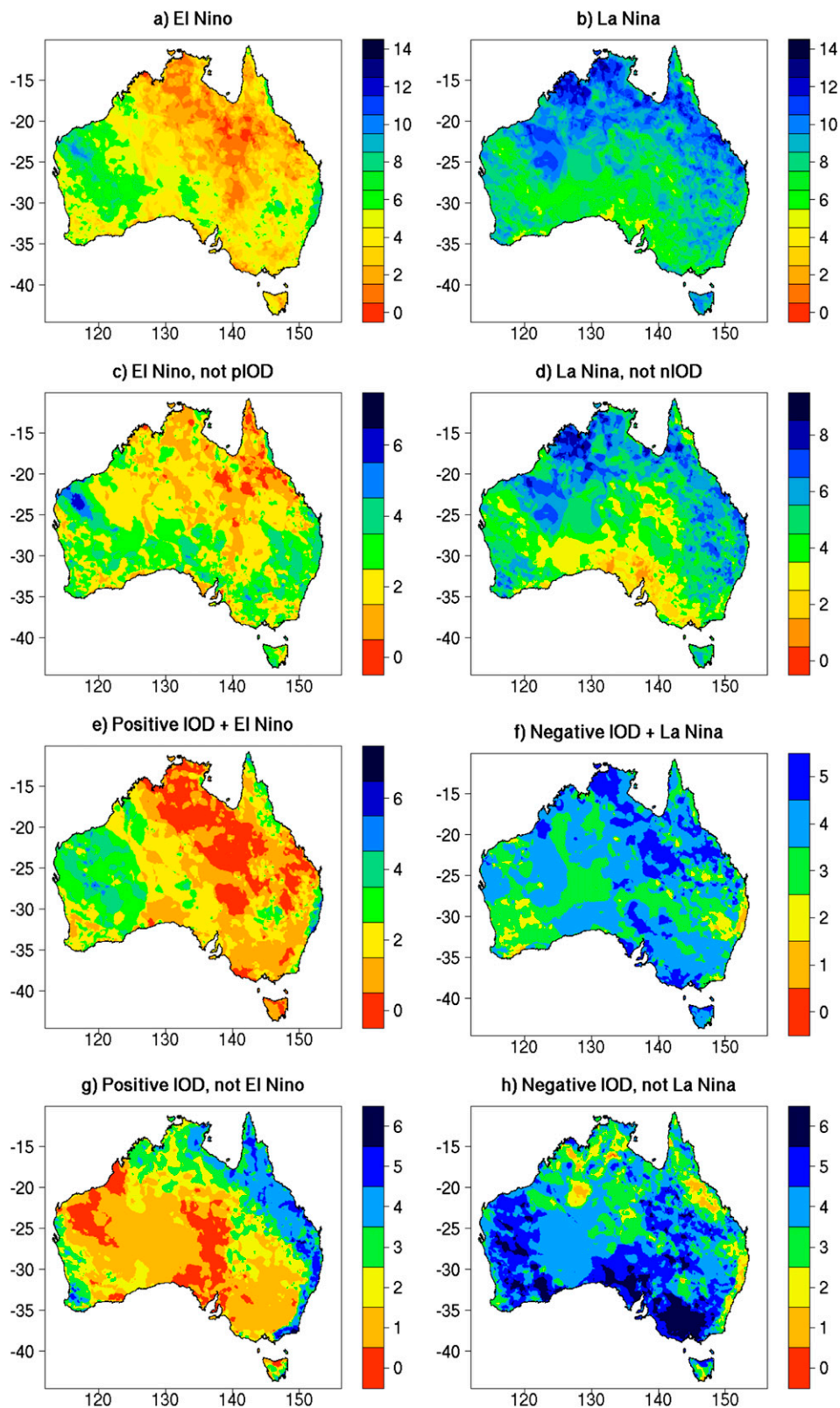


FIG. 8. Number of years between 1958 and 2012 with above-median June–October rainfall for various combinations of IOD–ENSO state (using BoM classification; Table 1). Note that the cases of 1993, 2007, and 2011, where the IOD and ENSO state were opposite, are counted twice.

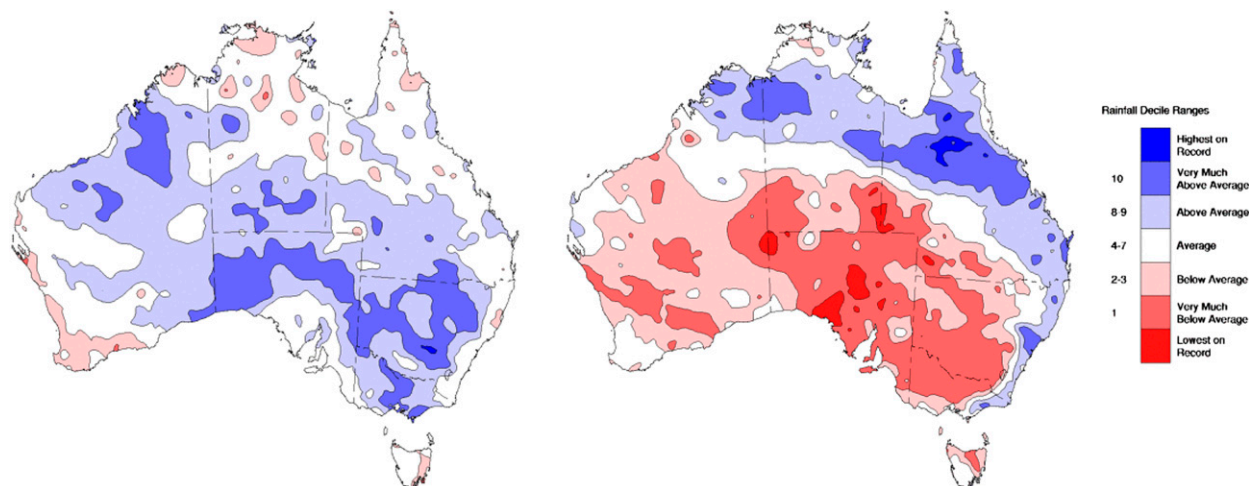


FIG. 9. Australian rainfall deciles for June–October during the anomalous years (left) 1993 (El Niño and nIOD) and (right) 2007 (La Niña and pIOD).

when both IOD and ENSO work in concert (Figs. 8e,f); this is to be expected from the strengthened moisture fluxes in the northern continent observed in Fig. 7. On the east coast, such combined events have minimal rainfall impact, with the enhanced moisture fluxes into the continent associated with ENSO events counteracted by the changes in zonal wind flow associated with the IOD. We postulate that during combined events, the enhanced moist southeasterly wind flow onto the ESB produced by positive IOD effectively replaces the diminished rainfall of weakened westerlies and a reduced frequency of cutoff lows and fronts caused by El Niño. This effective counterbalance explains the lack of correlation between the tropical indices and ESB cool season rainfall.

In years where the IOD and ENSO are out of phase, such as 1993 and 2007, the rainfall pattern in SEA during June–October is consistent solely with that expected of the IOD phase. That is, negative IOD produced enhanced rainfall west of the divide and drier conditions over the ESB (Fig. 9, left). Conversely, positive IOD produced dry conditions west of the divide and enhanced rainfall over the ESB in 2007 (Fig. 9, right), with similar rainfall patterns in 2011 (not shown). This further demonstrates the dominance of the IOD over both ENSO influences and the cool season climate of SEA. However, in both of these cases, the ENSO event was atypical; the 2007 and 2011 La Niña events both developed during late spring, following the season of peak IOD influence, while the 1993 El Niño was associated with only weak SST anomalies.

Finally, when the influence of IOD is removed, the partial correlation coefficients between Niño-3.4 and June–October rainfall across the eastern seaboard bear

strong similarities to those observed during the warm months November–March, consistent with patterns shown in Risbey et al. (2009b). In the absence of the IOD, both the cool and warm seasons exhibit enhanced rainfall in northeast Australia during La Niña years, with no weakening of correlations on the east coast (Fig. 10). This relationship is likely associated with the tropical teleconnection pathway discussed in Cai et al. (2011), through influences on SSTs and moisture flux around the northeast Australian continent. It is thus proposed that the presence of the IOD, and its clear influence on subtropical zonal wind anomalies, is the dominant cause of the sharply contrasted cool season rainfall patterns observed between the ESB and the vast plains west of the divide.

## 6. Conclusions

This paper builds on previous work into southeast Australian rainfall and the IOD (e.g., Meyers et al. 2007; Ummenhofer et al. 2009a,b, 2011; Risbey et al. 2009a,b; Cai et al. 2011, 2012) to provide a simple but powerful explanation for the lack of an observed relationship between ENSO and Australian rainfall along the east coast.

During the cool season, June–October, the prevailing wind direction and moisture flux across southern Australia is westerly. Enhancement of this westerly flow is associated with increased rainfall across the majority of southern Australia but decreased rainfall over the coastal strip to the east of the Great Dividing Range.

Using ENSO and the IOD to separate the complex influence of the tropical oceans, IOD events were found to be the dominant influences on ESB cool season

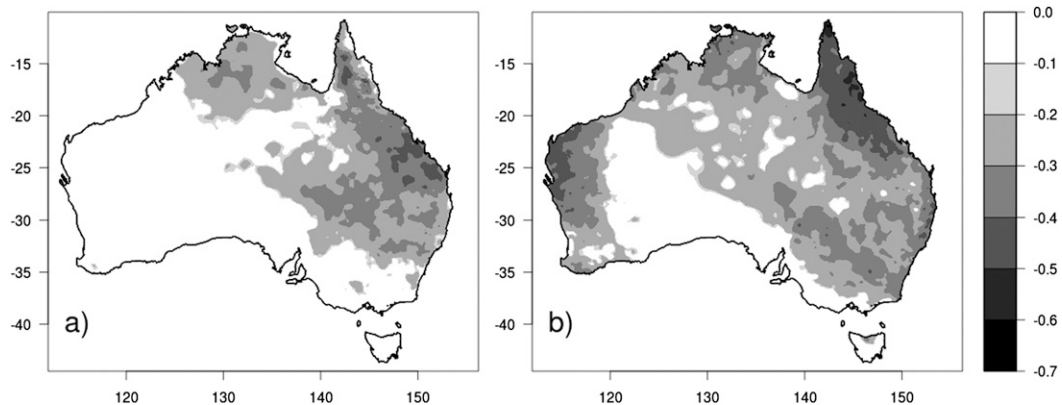


FIG. 10. (a) Partial correlation between Niño-3.4 and Australian rainfall in the absence of DMI, June–October 1900–2012; (b) November–March correlation between Niño-3.4 and Australian rainfall, 1900–2012. Only correlations that are statistically significant at the 95% level are shown.

rainfall, through enhancing or weakening this prevailing westerly flow. Consequently, in the absence of an ENSO event, the relationships between IOD and rainfall east of the Great Dividing Range are the inverse of those observed elsewhere in southeast Australia. In contrast, when the influence of IOD was removed, El Niño events were found to have no consistent influence on Australian moisture fluxes or rainfall, consistent with earlier results (Ummenhofer et al. 2009a), despite strong negative anomalies during some El Niño years such as 2002 and 2009. La Niña events were associated with increased moisture fluxes into eastern Australia and broadly enhanced rainfall in the northeast of the country, regardless of IOD.

The interaction between ENSO and the IOD is complex, with the strongest rainfall anomalies in Australia generally observed in years where both drivers act in concert (e.g., Ummenhofer et al. 2009a; Meyers et al. 2007). However, this study suggests that the interaction between ENSO and the IOD is also responsible for the observed lack of correlation between ESB rainfall and ENSO. This result also explains the strengthened relationship between La Niña events and east coast rainfall during the warm months (November–March), when the absence of the IOD's effects results in enhanced rainfall on the east coast of Australia. Further research will be needed into the dynamics of this relationship, particularly with respect to the interactions between ENSO and IOD, which this paper has simplified in order to identify their independent effects.

It is important to remember that the interplay of ENSO and the IOD is not the only influence on eastern seaboard rainfall; notably, east coast lows can produce very heavy coastal rainfall but have little relationship with either ENSO or the IOD, so they can further act to confound expected relationships through increasing

variability (e.g., Pepler et al. 2014). Nonetheless, the results presented in this paper clearly demonstrate the critical significance of the IOD in determining the rainfall impacts of tropical climate variability in southeast Australia, especially on the eastern seaboard.

*Acknowledgments.* The authors thank Scott Power, Harry Hendon, and two anonymous reviewers for their helpful comments, which have improved the clarity of this paper significantly.

## REFERENCES

- Brown, J. N., P. C. McIntosh, M. J. Pook, and J. S. Risbey, 2009: An investigation of the links between ENSO flavors and rainfall processes in southeastern Australia. *Mon. Wea. Rev.*, **137**, 3786–3795, doi:10.1175/2009MWR3066.1.
- Cai, W., P. van Rensch, T. Cowan, and H. Hendon, 2011: Teleconnection pathways of ENSO and the IOD and the mechanisms for impacts on Australian rainfall. *J. Climate*, **24**, 3910–3923, doi:10.1175/2011JCLI4129.1.
- , —, —, and H. H. Hendon, 2012: An asymmetry in the IOD and ENSO teleconnection pathway and its impact on Australian climate. *J. Climate*, **25**, 6318–6329, doi:10.1175/JCLI-D-11-00501.1.
- Hendon, H. H., D. W. J. Thompson, and M. C. Wheeler, 2007: Australian rainfall and surface temperature variations associated with the Southern Hemisphere annular mode. *J. Climate*, **20**, 2452–2467, doi:10.1175/JCLI4134.1.
- Jones, D. A., and B. C. Trewin, 2000: On the relationships between the El Niño–Southern Oscillation and Australian land surface temperature. *Int. J. Climatol.*, **20**, 697–719, doi:10.1002/1097-0088(20000615)20:7<697::AID-JOC499>3.0.CO;2-A.
- , W. Wang, and R. Fawcett, 2009: High-quality spatial climate data-sets for Australia. *Aust. Meteor. Ocean. J.*, **58**, 233–248.
- Kalnay, E., and Coauthors, 1996: The NCEP–National Center for Environmental Prediction 40-Year Reanalysis Project. *Bull. Amer. Meteor. Soc.*, **77**, 437–471, doi:10.1175/1520-0477(1996)077<0437:TNYRP>2.0.CO;2.
- McBride, J., and N. Nicholls, 1983: Seasonal relationships between Australian rainfall and the Southern Oscillation. *Mon. Wea.*

- Rev.*, **111**, 1998–2004, doi:10.1175/1520-0493(1983)111<1998:SRBARA>2.0.CO;2.
- McIntosh, P. C., J. S. Risbey, J. N. Brown, and M. J. Pook, 2012: Apparent and real sources of rainfall associated with a cutoff low in southeast Australia. *CAWCR Research Letters*, No. 8, CAWCR, Melbourne, Australia, 4–9. [Available online at [www.cawcr.gov.au/publications/researchletters/CAWCR\\_Research\\_Letters\\_8.pdf](http://www.cawcr.gov.au/publications/researchletters/CAWCR_Research_Letters_8.pdf).]
- Meyers, G., P. McIntosh, L. Pigot, and M. Pook, 2007: The years of El Niño, La Niña, and interactions with the tropical Indian Ocean. *J. Climate*, **20**, 2872–2880, doi:10.1175/JCLI4152.1.
- Nicholls, N., 1985: Impact of the Southern Oscillation on Australian crops. *Int. J. Climatol.*, **5**, 553–560, doi:10.1002/joc.3370050508.
- Pepler, A. S., A. Coutts-Smith, and B. Timbal, 2014: The role of east coast lows on rainfall patterns and inter-annual variability across the east coast of Australia. *Int. J. Climatol.*, **34**, 1011–1021, doi: 10.1002/joc.3741.
- Power, S., F. Tseitkin, S. J. Torok, B. Lavery, R. Dahni, and B. McAvaney, 1998: Australian temperature, Australian rainfall and the Southern Oscillation, 1910–1992: Coherent variability and recent changes. *Aust. Meteor. Mag.*, **47**, 85–101.
- Rakich, C. S., N. J. Holbrook, and B. Timbal, 2008: A pressure gradient metric capturing planetary-scale influences on eastern Australian rainfall. *Geophys. Res. Lett.*, **35**, L08713, doi:10.1029/2007GL032970.
- Rayner, N. A., P. Brohan, D. E. Parker, C. K. Folland, J. J. Kennedy, M. Vanicek, T. Ansell, and S. F. B. Tett, 2006: Improved analyses of changes and uncertainties in sea surface temperature measured in situ since the mid-nineteenth century: The HadSST2 data set. *J. Climate*, **19**, 446–469, doi:10.1175/JCLI3637.1.
- Risbey, J. S., M. J. Pook, P. C. McIntosh, C. C. Ummenhofer, and G. Meyers, 2009a: Characteristics and variability of synoptic features associated with cool season rainfall in southeastern Australia. *Int. J. Climatol.*, **29**, 1595–1613, doi:10.1002/joc.1775.
- , —, —, M. C. Wheeler, and H. H. Hendon, 2009b: On the remote drivers of rainfall variability in Australia. *Mon. Wea. Rev.*, **137**, 3233–3253, doi:10.1175/2009MWR2861.1.
- Saji, N. H., B. N. Goswami, P. N. Vinayachandran, and T. Yamagata, 1999: A dipole mode in the tropical Indian Ocean. *Nature*, **401**, 360–363.
- Speer, M. S., L. M. Leslie, and A. O. Fierro, 2011: Australian east coast rainfall decline related to large scale climate drivers. *Climate Dyn.*, **36**, 1419–1429, doi:10.1007/s00382-009-0726-1.
- Taschetto, A. S., A. Sen Gupta, H. H. Hendon, C. C. Ummenhofer, and M. H. England, 2011: The contribution of Indian Ocean sea surface temperature anomalies on Australian summer rainfall during El Niño events. *J. Climate*, **24**, 3734–3747, doi:10.1175/2011JCLI3885.1.
- Timbal, B., 2010: The climate of the eastern seaboard of Australia: A challenging entity now and for future projections. *IOP Conf. Ser.: Earth Environ. Sci.*, **11**, 012013, doi:10.1088/1755-1315/11/1/012013.
- , and H. Hendon, 2011: The role of tropical modes of variability in recent rainfall deficits across the Murray-Darling Basin. *Water Resour. Res.*, **47**, W00G09, doi:10.1029/2010WR009834.
- Trenberth, K. E., 1997: The definition of El Niño. *Bull. Amer. Meteor. Soc.*, **78**, 2771–2777, doi:10.1175/1520-0477(1997)078<2771:TDOENO>2.0.CO;2.
- Ummenhofer, C. C., M. H. England, P. C. McIntosh, G. A. Meyers, M. J. Pook, J. S. Risbey, A. S. Gupta, and A. S. Taschetto, 2009a: What causes southeast Australia's worst droughts? *Geophys. Res. Lett.*, **36**, L04706, doi:10.1029/2008GL036801.
- , A. S. Gupta, A. S. Taschetto, and M. H. England, 2009b: Modulation of Australian precipitation by meridional gradients in east Indian Ocean sea surface temperature. *J. Climate*, **22**, 5597–5610, doi:10.1175/2009JCLI3021.1.
- , and Coauthors, 2011: Indian and Pacific Ocean influences on southeast Australian drought and soil moisture. *J. Climate*, **24**, 1313–1336, doi:10.1175/2010JCLI3475.1.